Fastest first-passage time statistics for time-dependent particle injection

Denis S. Grebenkov [1,*] Ralf Metzler [2,3] and Gleb Oshanin [4,3]

[1]*Laboratoire de Physique de la Matière Condensée, CNRS–Ecole Polytechnique, Institut Polytechnique de Paris, 91120 Palaiseau, France*
[2]*Institute for Physics & Astronomy, University of Potsdam, 14476 Potsdam-Golm, Germany*
[3]*Asia Pacific Center for Theoretical Physics, Pohang 37673, Republic of Korea*
[4]*Sorbonne Université, CNRS, Laboratoire de Physique Théorique de la Matière Condensée (UMR CNRS 7600),
4 Place Jussieu, 75252 Paris Cedex 05, France*

A common scenario in a variety of biological systems is that multiple particles are searching in parallel for an immobile target located in a bounded domain, and the fastest among them that arrives to the target first triggers a given desirable or detrimental process. The statistics of such extreme events—the *fastest* first-passage to the target—is well-understood by now through a series of theoretical analyses, but exclusively under the assumption that all N particles start *simultaneously*, i.e., all are introduced into the domain instantly, by δ-function-like pulses. However, in many practically important situations this is not the case: to start their search, the particles often have to enter first into a bounded domain, e.g., a cell or its nucleus, penetrating through gated channels or nuclear pores. This entrance process has a random duration so that the particles appear in the domain sequentially and with a time delay. Here we focus on the effect of such an extended-in-time injection of multiple particles on the fastest first-passage time (fFPT) and its statistics. We derive the full probability density function $H_N(t)$ of the fFPT with an arbitrary time-dependent injection intensity of N particles. Under rather general assumptions on the survival probability of a single particle and on the injection intensity, we derive the large-N asymptotic formula for the mean fFPT, which is quite different from that obtained for the instantaneous δ-pulse injection. The extended injection is also shown to considerably slow down the convergence of $H_N(t)$ to its large-N limit—the Gumbel distribution—so that the latter may be inapplicable in the most relevant settings with few tens to few thousands of particles.

I. INTRODUCTION

"The winner takes it all" situation, in which the fastest of many actors produces a required action, is realized in diverse processes in physiology, neuroscience, and cellular biology. For instance, 300 million motile sperms search for the egg cell, and the first among them joins an ovum to form a zygote [1]. Many thousands of cells (e.g., bacteria) in a colony compete with each other to first respond to a common environmental challenge [2,3]. In cellular processes, a large amount of messengers speedup and control signal transduction and cell communication; e.g., the fastest among several hundreds of calcium ions injected into a dendritic spine triggers a transduction, while several thousands of neurotransmitters diffusing in the presynaptic terminal search for receptors on the post-synaptic membrane [4,5]. In the cell nucleus, many transcription factors seek in parallel a specific binding site on the cellular DNA [6]. Further examples can be found in a recent monograph [7].

---

*Contact author: denis.grebenkov@polytechnique.edu

In the mathematical modeling of these processes (see, e.g., Refs. [8–18]), a common theme is to suppose that all particles are injected into the domain simultaneously, by δ-function-like pulses. This is tantamount to the tacit assumption that the duration of the injection process is much shorter than the typical timescales of the subsequent search processes—certainly a plausible scenario in the case of the sperm cells, but not in general. In particular, transcription factors in cells typically do not start at the same time instant but are produced in intermittent bursts and/or at different locations [6,19,20] as well as do not spread evenly over the cell [21,22]. In the case of viral infections, the viruses may keep on entering a single living cell, or injecting their RNA/DNA into it, within significantly extended periods of time [23]. Similarly, the injection of ions into a cell through gated channels is typically spread over time [24,25]. Such channels—molecular machines (see Fig. 1) [5], which transport ions through the cell membrane with high efficiency of 10^6–10^8 ions/s—are typically open for a few milliseconds. As the diffusion coefficient of an ion in the cytoplasm is typically of the order of a few tens of $\mu m^2/s$, the first ion entering the cell may diffuse away from the point of injection on quite noticeable distances of a few hundreds of nanometers, before the last ion in the pulse even enters the cell. Since the typical reaction times themselves are often of order of milliseconds, or even much shorter—as in case of diffusion-controlled reaction of a single calcium
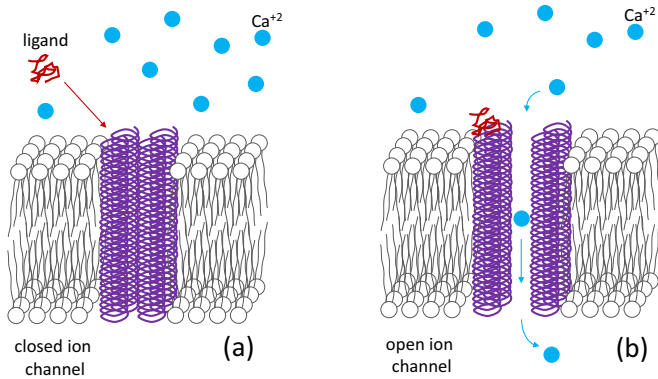
023239-1

FIG. 1. Illustration of a sequential influx of calcium ions into a cell through an ion channel. In panel (a) the channel is closed while panel (b) depicts a channel, which opens due to the arrival of a ligand to a special binding site [5].

ion to a calcium-sensor protein [26–30]—the reaction event may take place well before the last ion enters the cell. In consequence, only some portion of the injected ions will effectively contribute to the search process such that the fastest first-passage time (fFPT) to the reaction event and other characteristic timescales, calculated using the assumption of an injection via a δ pulse, may considerably underestimate the actual characteristics of these properties and therefore present an inadequate picture of the kinetic behavior. Moreover, one can even aim at optimizing the search process by adjusting the injection rate or injecting individual searchers at prescribed time instances [31,32].

Here, we combine analytical and numerical tools to address the conceptually important question on how the duration of the injection stage or, more specifically, the time dependence of the injection intensity $\psi(t)$ affects the statistics of the fFPT to the reaction event—and how different it can be from the one corresponding to the situation when all N particles are simultaneously injected to the reaction bath by a δ-pulse. We derive exact expressions for the probability density function (PDF) of the fFPT for a general time-dependent injection profile $\psi(t)$. Next, we analyze how the form of $\psi(t)$ affects the asymptotic large-N behavior of the mean fFPT and of the full fFPT-PDF. In particular, we demonstrate that an extended-in-time injection drastically slows down the convergence of the fFPT-PDF to the Gumbel distribution, which is the fingerprint feature of the δ-pulse injection [12–17].

The paper is outlined as follows. In Sec. II we formulate our model and introduce general notations as well as define two basic injection scenarios. Section III contains our theoretical results. In particular, Sec. III D presents the large-N asymptotic behavior of the mean fFPT for an extended-in-time particle injection and discusses three possible regimes according to the injection profile. Section IV is dedicated to a numerical validation of our predictions for a particular case of one-dimensional diffusion. Finally, in Sec. VI we conclude with a brief summary of our results. Details of intermediate calculations are relegated to Appendixes.

II. MODEL AND NOTATIONS

Consider a bounded domain in which N particles are sequentially injected at some fixed time instants $\delta_1, \delta_2, \ldots, \delta_N$. Note that all particles may appear in the domain at the same location, e.g., corresponding to the passage through a single ion channel (see Fig. 1), as it was assumed in Refs. [12–18]. Alternatively, the starting points can be drawn from a given spatial distribution, e.g., it can be uniformly distributed on the plasma membrane as it happens when viruses are penetrating into the cell [23,33]. All derivations below remain valid for both cases, but we stress that the behavior of the fFPT may strongly depend on the precise spatial distribution of the starting points.

We assume that the domain contains a target site which the N particles are searching for *independently* of each other. Let $\tau_k + \delta_k$ denote the random time instant when the kth particle reaches the target for the first time and let $S(t - \delta_k)$ (with the convention $S(t \leqslant 0) \equiv 1$) denote the corresponding "survival" probability, i.e., the probability that the kth particle did not arrive to the target within the time interval $t - \delta_k$. Note that since the domain is bounded, one evidently has $S(t) \to 0$ as $t \to \infty$, such that any particle is *certain* to find the target. Then, denoting the fFPT as

$$\mathcal{T}_N = \min\{\tau_1 + \delta_1, \ldots, \tau_N + \delta_N\}, \qquad (1)$$

one writes the probability that none of the N particles has reached the target up to time t as

$$\mathbb{P}\{\mathcal{T}_N > t\} = \prod_{k=1}^{N} S(t - \delta_k), \qquad (2)$$

for a given set of time instants $\delta_1, \delta_2, \ldots, \delta_N$. In what follows, we consider two possible scenarios with respect to the variables δ_k:

(A) *Deterministic injection.* In this scenario we assume that a fraction $N\psi(t)dt$ of particles enters the domain within the time interval $(t, t + dt)$, with a given flux profile $\psi(t)$ per particle.

(B) *Random injection.* Here, we suppose that δ_k are independent, identically distributed random variables with common probability density $\psi(t)$.

For both scenarios, the survival probability $S_N(t)$ of the target in the presence of N particles with a time-extended injection is obtained by averaging the probability $\mathbb{P}\{\mathcal{T}_N > t\}$ with respect to the distribution of the variables δ_k. Correspondingly, the PDF $H_N(t)$ of the fFPT is the time-derivative of $S_N(t)$, taken with the negative sign,

$$H_N(t) = -\frac{dS_N(t)}{dt}, \qquad (3)$$

while the mean fFPT obeys

$$\langle \mathcal{T}_N \rangle = \int_0^\infty dt\, t\, H_N(t) = \int_0^\infty dt\, S_N(t). \qquad (4)$$

Note, as well, that for situations in which the particles start from random positions, the survival probability $S(t)$ is supposed to already include this spatial average.

III. ANALYTICAL RESULTS

A. Deterministic injection

For the deterministic injection scenario, the formal expression (2) is neither suitable for the asymptotic analysis for large N, nor for the analytical inspection of the role of the entrance delays. To overcome this limitation, we describe the noninstantaneous injection of particles by introducing a piecewise-constant function $N(t)$ that increases by unity at each injection event and counts the number of particles that have entered up to time t. When N is large, it is more convenient to "smooth" the rescaled profile $\eta(t) = N(t)/N$, i.e., to consider it as a smooth function of time which increases from zero at $t = 0$ to unity in the limit $t \to \infty$. We can therefore define the influx of particles at time t as $\psi(t) = d\eta(t)/dt$, so that $N\psi(t)\delta$ is the "number" of particles having entered the domain during a short time period from t to $t + \delta$. In doing so, one finds

$$\langle \mathbb{P}\{\mathcal{T}_N > t\}\rangle_{\delta_k} \approx [S(t)]^{N\psi(0)\delta} [S(t-\delta)]^{N\psi(\delta)\delta} \ldots [S(0)]^{N\psi(t)\delta},$$

$$(5)$$

where the brackets denote averaging over the entrance times $\delta_1, \ldots, \delta_N$. In the continuous limit $\delta \to 0$, the product on the right-hand side converges to the expression

$$\langle \mathbb{P}\{\mathcal{T}_N > t\}\rangle_{\delta_k} \xrightarrow[\delta \to 0]{} \bar{S}_N(t) = [\bar{S}_\psi(t)]^N, \qquad (6)$$

where $\bar{S}_N(t)$ denotes the survival probability of the target in the presence of N particles injected into the domain with the smooth time-dependent injection profile $\psi(t)$, and

$$\bar{S}_\psi(t) = \exp\left(\int_0^t dt'\, \psi(t') \ln S(t-t')\right). \qquad (7)$$

As a consequence, we find for the deterministic injection that

$$\bar{S}_N(t) = \exp\left(N \int_0^t dt'\, \psi(t') \ln S(t-t')\right). \qquad (8)$$

Respectively, in virtue of Eq. (3), the fFPT-PDF obeys

$$\bar{H}_N(t) = -\frac{d}{dt}[\bar{S}_\psi(t)]^N, \qquad (9)$$

while the mean fFPT, by virtue of Eq. (4), is determined by the integral

$$\langle \bar{\mathcal{T}}_N \rangle = \int_0^\infty dt\, [\bar{S}_\psi(t)]^N. \qquad (10)$$

Note that in the limit $N \to \infty$ the integral in the latter expression is evidently dominated by the behavior of $\bar{S}_\psi(t)$ and, hence, of $\psi(t)$ in the vicinity of $t = 0$.

Two remarks are in order:

(i) One can easily show that $\bar{S}_\psi(t)$ is a positive function that monotonously decreases from unity at $t = 0$ to zero as $t \to \infty$ (see Appendix A). As a consequence, one can interpret $\bar{S}_\psi(t)$ as the survival probability of an effective particle whose diffusive search for the target already incorporates the delayed entrance. In other words, one can introduce an effective FPT $\bar{\tau}_k$ via $\bar{S}_\psi(t) = \mathbb{P}\{\bar{\tau}_k > t\}$ that accounts for the extended injection. In this way, the search by the particles that were injected progressively via the profile $\psi(t)$, is equivalent to the search

by the effective particles injected instantaneously, i.e., the distribution of the fFPT $\mathcal{T}_N$ is getting close to $\mathbb{P}\{\bar{\mathcal{T}}_N > t\} = \bar{S}_N(t)$ of the minimum $\bar{\mathcal{T}}_N = \min\{\bar{\tau}_1, \ldots, \bar{\tau}_N\}$ for large N.

(ii) For an instantaneous injection of N particles with a δ-pulse, one has $\psi(t) \equiv \delta(t)$, so that $\bar{S}_\psi(t) \equiv S(t)$, i.e., the survival probability of the target in the presence of just a single searcher. This gives straightforwardly $\bar{S}_N(t) = [S(t)]^N$, i.e., the standard starting point of the analyses of the fFPTs in systems with instantaneously generated N particles [8,12–18]. We will comment on the results of these analyses in what follows, comparing them with our theoretical findings for an extended-in-time injection.

B. Random injection

In this scenario, we consider the entrance times δ_k as independent and identically distributed random variables governed by the PDF $\psi(t)$, which is determined by a given injection profile. Due to the factorized form of Eq. (2), the averaging of this expression over the variables δ_k can be performed straightforwardly, yielding

$$\langle \mathbb{P}\{\mathcal{T}_N > t\}\rangle_{\delta_k} = S_N(t) = [S_\psi(t)]^N, \qquad (11)$$

where

$$\begin{aligned} S_\psi(t) &= \int_0^\infty dt'\, \psi(t') S(t-t') \\ &= \int_0^\infty dt'\, \psi(t') - \int_0^\infty dt'\, \psi(t')[1 - S(t-t')] \\ &= 1 - \int_0^t dt'\, \psi(t')[1 - S(t-t')], \qquad (12) \end{aligned}$$

where we took advantage of the fact that $S(t < 0) = 1$. This relation also implies

$$H_\psi(t) = \int_0^t dt'\, \psi(t') H(t-t'), \qquad (13)$$

as expected for the sum $\tau_k + \delta_k$ of two independent random variables. Consequently, in virtue of Eq. (3), the fFPT-PDF in this scenario obeys

$$H_N(t) = -\frac{d}{dt}[S_\psi(t)]^N, \qquad (14)$$

while the mean fFPT is determined by the integral

$$\langle \mathcal{T}_N \rangle = \int_0^\infty dt\, [S_\psi(t)]^N. \qquad (15)$$

Consequently, in the limit $N \to \infty$ the integral in Eq. (15) is also dominated by the behavior of $S_\psi(t)$ and, hence, of $\psi(t)$ in the vicinity of $t = 0$. This is the reason why, although the random injection is formally different from the deterministic injection, the results of both injection scenarios will appear very similar in the limit of large N, as we proceed to show in the following.

C. Asymptotic behavior for instantaneous injection

To set the scene, we first briefly recall the main results corresponding to the situation in which all particles are simultaneously injected into the domain and then move independently of each other, searching in parallel for a given

immobile target. Note that the notations and the main equations presented in Sec. II are valid in this case and correspond to the choice $\psi(t) = \delta(t)$. To avoid confusion, we add the superscript "0" when referring to the characteristic properties in this case, such as the mean fFPT $\mathcal{T}_N^0$, the survival probability $S_N^0(t)$ and the fFPT-PDF $H_N^0(t)$.

In the context of the diffusive motion of particles in a one-dimensional system, the statistics of the mean fFPT for simultaneous injection of N particles was first addressed by Weiss *et al.* [8], who revealed the extremely slow dependence of the mean fFPT on the number of particles,

$$\langle \mathcal{T}_N^0 \rangle \simeq \frac{C}{\ln N} \quad (N \to \infty), \tag{16}$$

where $C = \ell^2/(4D)$ is the natural timescale of the search process, expressed in terms of the diffusion coefficient D and the distance ℓ between the starting point and the target. Therefore, the speedup of the search process due to multiple independent particles starting simultaneously from the same point turns out to be minor, an observation which provoked speculations why the numbers of searchers employed in diverse processes in biology and physiology are typically so high (the so-called "redundancy principle") [10].

Many other aspects of this challenging problem were also discussed in this seminal paper [8]. Several extensions and more elaborate descriptions were presented in subsequent works [11–16], including, e.g., the analysis of the statistics of the kth fastest FPT and its higher-order and joint moments, as well as a generalisation of the asymptotic result (16) for diffusion in higher-dimensional spaces. Moreover, it was demonstrated that in the large N limit, the fFPT-PDF converges to the universal Gumbel distribution, with nonuniversal, dynamic-specific scale and location parameters a_N and b_N [12]. The large-N asymptotic behavior of these parameters, as well as that of the fFPT moments, appears to be quite elaborate and completely dominated by the short-time behavior of the survival probability $S(t)$. In particular, Lawley derived the asymptotic expressions for a_N and b_N and thus for the mean and the variance of the fFPT under the rather general assumption on the short-time asymptotic behavior of the survival probability,

$$1 - S(t) \sim A t^{\alpha} e^{-C/t} \quad (t \to 0), \tag{17}$$

with the constants $A > 0$ and $C > 0$, and $\alpha \in \mathbb{R}$ [12]. We note parenthetically that the expression for the mean fFPT in Eq. (16) stems from the exponentially fast decay of $1 - S(t)$ above, while the precise value of the exponent α in the preexponential factor is less important. In turn, it was shown that if the initial particle distribution is uniform, the mean fFPT scales as $1/N^2$ for perfect reactions upon the first arrival to the target, and as $1/N$ for the case of finite reactivity [15,16], entailing a much more significant speedup of the search process—as compared to the $1/\ln N$ law, which occurs when all particles start from the same location. We finally note that interactions between particles or correlations between their first-passage times may totally change the statistics of the fFPT (see [34,35] and references therein).

D. Asymptotic behavior for extended injection

Returning to the case of an extended-in-time injection, we focus on the limit $N \to \infty$, for which the behavior of the mean fFPT is entirely dominated by the short-time behavior of the survival probabilities $\bar{S}_\psi(t)$ and $S_\psi(t)$ and, hence, by the form of the injection profile $\psi(t)$ in the vicinity of $t = 0$. Assuming that $\psi(t)$ originates from a random transport process, e.g., the random motion of particles within a nuclear pore or an ion channel, we stipulate here that it has the quite generic form

$$\psi(t) \approx a t^{\nu-1} e^{-(c/t)^{\mu}} \quad (t \to 0), \tag{18}$$

with strictly positive constants a and c and exponents ν and $\mu \geqslant 0$. In Appendix B, we show the equivalence of $\bar{S}_\psi(t)$ and $S_\psi(t)$ to leading order for the large-N limit, such that it suffices to consider either of these quantities. This implies that the mean fFPTs in both scenarios, defined in Eqs. (10) and (15), are equal to each other to leading order: $\langle \bar{\mathcal{T}}_N \rangle = \langle \mathcal{T}_N \rangle$, as $N \to \infty$. Moreover, we find the following asymptotic behavior (see Appendix B for more details)

$$1 - S_\psi(t) \approx \bar{A} t^{\bar{\alpha}} e^{-(\bar{C}/t)^{\bar{\mu}}} \quad (t \to 0), \tag{19}$$

where the coefficients $\bar{A}$, $\bar{C}$, $\bar{\alpha}$, and $\bar{\mu}$ are determined by the parameters in Eqs. (17) and (18), as will be discussed below. Note that the crucial parameter $\bar{\mu}$ is given by the value of the exponent that characterizes the more singular behavior of the search dynamics: either the time-extended injection process $\psi(t) \sim \exp(-1/t^{\mu})$, or the diffusive transport of particles to the target, $1 - S(t) \sim \exp(-1/t^{\eta})$ (with $\eta = 1$); in fact, it controls the overall behavior of the survival probability $S_\psi(t)$ in the limit $t \to 0$. We also note parenthetically that $\eta = 1$ is a fingerprint feature of Brownian motion but η may differ from unity for anomalous diffusion dynamics. In particular, for any Gaussian process the exponent η characterizing the singularity in the short-t asymptotic of the FPT-PDF and, hence, of the survival probability, coincides with the so-called anomalous diffusion exponent [36]. Clearly, in the challenging and sometimes more physically realistic case of anomalous diffusion, which takes place at least at sufficiently short times, one will encounter a much richer scenario than in the case of a Brownian motion. Below we restrict our analysis to the case of Brownian motion, showing that even in this simpler case three different scenarios may be distinguished.

The asymptotic behavior (19) determines the large-N limit of the mean fFPT and related quantities. We sketch here simple arguments for the mean fFPT $\langle \mathcal{T}_N \rangle$ that can be made more rigorous and further extended by the asymptotic tools discussed in Refs. [8,12]. The function $S_N(t) = [S_\psi(t)]^N$ is a monotonically decreasing function of t such that the integral in Eq. (15) is dominated by the region in the vicinity of $t = 0$. This function is also a monotonically decreasing function of N, which implies that the region around $t = 0$ shrinks upon increase of N. In a first approximation, one can evaluate the integral in Eq. (15) by replacing $[S_\psi(t)]^N$ by a Heaviside step function, $\Theta(T - t)$, which is equal to unity for $t < T$ and zero otherwise. The mean fFPT is thus approximately equal to the cutoff value T delimiting the range $(0, T)$ of the contributing times which can be set by the condition $[S_\psi(T)]^N = 1 - q_0$, where q_0 is an auxiliary parameter determining a "sufficient" drop of $[S_\psi(t)]^N$. Substituting into

Eq. (19), one finds $\bar{A}T^{\bar{\alpha}}\exp(-(\bar{C}/T)^{\bar{\mu}}) \approx 1 - (1-q_0)^{1/N} \approx q/N$, for sufficiently large N; here, $q = -\ln(1-q_0)$. An approximate solution of this transcendental equation can be found perturbatively by taking the logarithm such that

$$\langle \mathcal{T}_N \rangle \approx T \approx \frac{\bar{C}}{[\ln(N) + \alpha\ln(T) + \ln(\bar{A}/q)]^{1/\bar{\mu}}}$$
$$\approx \frac{\bar{C}}{(\ln N)^{1/\bar{\mu}}}\left(1 + \frac{\frac{\bar{\alpha}}{\bar{\mu}}\ln\ln N - \ln(\bar{A}\bar{C}^{\bar{\alpha}}/q)}{\bar{\mu}\ln N}\right),$$

where $\ln(T)$ in the denominator in the top equation was replaced by its leading-order expression $\ln(\bar{C}/(\ln N)^{1/\bar{\mu}})$. Importantly, the leading-order term does not depend on the somewhat arbitrary parameter q. For $\bar{\mu} = 1$, we retrieve the expression for the mean fFPT derived by Lawley for the instantaneous injection scenario via a considerably more elaborate and rigorous asymptotic analysis [12] (see also Appendix C). Moreover, if we choose $q = e^{-\gamma} \approx 0.5615$, where γ is the Euler constant, the correction term becomes identical to that of Lawley's rigorous expression, thus confirming that our rough approximation captures correctly the subtle behavior of the mean fFPT. In other words, our expansion

$$\langle \mathcal{T}_N \rangle \approx \frac{\bar{C}}{(\ln N)^{1/\bar{\mu}}}\left(1 + \frac{\frac{\bar{\alpha}}{\bar{\mu}}\ln\ln N - \ln(\bar{A}\bar{C}^{\bar{\alpha}}e^{\gamma})}{\bar{\mu}\ln N}\right) \qquad (20)$$

is reduced to the rigorous result by Lawley in the special case of an instantaneous injection.

The parameters $\bar{A}$, $\bar{C}$, $\bar{\alpha}$, and $\bar{\mu}$ in Eq. (19) can be expressed in terms of the parameters A, C, and α of the survival probability $S(t)$, and a, c, ν, and μ of the injection profile $\psi(t)$. Skipping technical details (see Appendix B), we draw the main conclusions for three different types of the injection profile:

(i) If $0 \leqslant \mu < 1$, then the survival probability $S(t)$ is the limiting factor such that

$$\bar{\mu} = 1, \quad \bar{C} = C, \qquad (21)$$

and the leading term $C/\ln N$ does not depend on the shape of the injection profile. The latter only affects the correction term through the coefficients $\bar{A}$ and $\bar{\alpha}$ given by Eqs. (B15) for $\mu = 0$ and by Eqs. (B11) for $0 < \mu < 1$.

(ii) If $\mu = 1$, then relations (17) and (18) exhibit similar asymptotic behaviors, yielding $\bar{\mu} = 1$ and $\bar{C} = (\sqrt{C} + \sqrt{c})^2$ for the coefficient in front of the leading term (the correction term also changes, see Eqs. (B9) for $\bar{A}$ and $\bar{\alpha}$).

(iii) If $\mu > 1$, then the profile $\psi(t)$ decreases faster than $1 - S(t)$ at short times such that the extended injection is the limiting factor for the fastest arrival to the target. In this case, the leading term of $\langle \mathcal{T}_N \rangle$ exhibits the even slower decrease of the form $\bar{C}/(\ln N)^{1/\bar{\mu}}$ with $\bar{C} = c$ and $\bar{\mu} = \mu$, which is independent of the diffusive dynamics, that only affects the correction term [see Eqs. (B7) for $\bar{A}$ and $\bar{\alpha}$].

In a similar way, one can analyze the higher-order moments of the fFPT-PDF for an extended injection. We restrict our attention to the case $0 \leqslant \mu \leqslant 1$, for which $\bar{\mu} = 1$ and thus the short-time asymptotic behavior of the survival probability $S_\psi(t)$ admits the same form as Eq. (17), upon replacing C, α, and A by $\bar{C}$, $\bar{\alpha}$, and $\bar{A}$, respectively. As a consequence, one

can apply the original result of Lawley for the instantaneous injection case (see Appendix C). In particular, if $\bar{\alpha} > 0$, the variance of the fFPT is given by

$$\mathrm{Var}\{\mathcal{T}_N\} \approx \frac{\pi^2}{6}\left(\frac{\bar{C}}{\bar{\alpha}^2\bar{W}(1+\bar{W})}\right)^2 \quad (N \gg 1), \qquad (22)$$

where

$$\bar{W} = W_0(\bar{C}(\bar{A}N)^{1/\bar{\alpha}}/\bar{\alpha}), \qquad (23)$$

and $W_0(z)$ is the principal branch of the Lambert W-function [12] (see Appendix C for other cases). For sufficiently large N, one can use the asymptotic behavior of this function to get

$$\mathrm{Var}\{\mathcal{T}_N\} \approx V_N, \quad V_N = \frac{\pi^2}{6}\frac{C^2}{(\ln N)^4} \quad (N \gg 1), \qquad (24)$$

i.e., the leading-order behavior of the variance is independent of the injection profile.

IV. NUMERICAL ANALYSIS OF A PARTICULAR EXAMPLE

To illustrate the above-discussed effects and to check the accuracy of the derived asymptotic relations, we consider diffusion in the upper half-space toward an absorbing plane (the target). As lateral displacements do not affect the transverse motion and thus the statistics of the first arrival onto the plane, this first-passage problem is equivalent to diffusion on the half-line $\Omega = (0, +\infty)$ from a fixed starting point $x_0 > 0$ toward an absorbing origin. In this prototypical setting, one has $S(t) = \mathrm{erf}(x_0/\sqrt{4Dt})$, where $\mathrm{erf}(z)$ is the error function, so that the asymptotic relation (17) holds, with

$$C = \frac{x_0^2}{4D}, \quad \alpha = \frac{1}{2}, \quad A = \frac{1}{\sqrt{\pi C}}. \qquad (25)$$

Despite the simplicity of this example, the underlying Lévy-Smirnov PDF $H(t) = -\frac{d}{dt}S(t) = x_0 e^{-x_0^2/(4Dt)}/\sqrt{4\pi Dt^3}$ captures well the short-time behavior of the FPT-PDF in various geometric settings, as well as in higher dimensions, and is thus a representative example for the large-N asymptotic behavior of the fFPT statistics.

In turn, the entrance times δ_k are modeled via the gamma distribution that corresponds to the injection profile

$$\psi(t) = \frac{t^{\nu-1}e^{-t/b}}{b^\nu\Gamma(\nu)}, \qquad (26)$$

with the shape parameter $\nu > 0$ and the scale parameter $b > 0$. This model obeys the short-time behavior (18) with $\mu = 0$ and $a = b^{-\nu}/\Gamma(\nu)$ so that this injection profile is supposed to have the *weakest* impact onto the fFPT [case (i)]; indeed, according to Eq. (21), the leading-order behavior of the mean fFPT remains unchanged. We have chosen this model to illustrate that even such a mild modification in the short-time asymptotic behavior of the survival probability $S_\psi(t)$ can produce significant alterations in the behavior of the fFPT. Figure 2 illustrates three injection profiles modeled by Eq. (26). Note that $\psi(t)$ formally converges to $\delta(t)$ in the limit $\nu \to 0$, corresponding to instantaneous injection. In the following, we mostly focus on the case $b = 1$ and $\nu = 5$ as a representative example. In
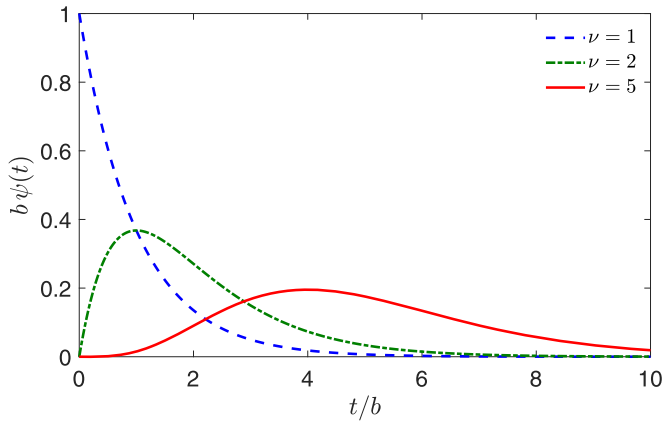
FIG. 2. Three injection profiles modeled by the gamma distribution (26), with the timescale $b = 1$ and three scale parameters ν indicated as in the legend.

Appendix D, we discuss another common injection profile when the delay times δ_k are uniformly distributed over an interval $(0, T)$. In this setting, we get exact explicit formulas for $H_\psi(t)$ and $S_\psi(t)$ and reveal the role of the shape of the injection profile.

To check the asymptotic relations, we need to compute numerically the mean fFPT $\langle \mathcal{T}_N \rangle$ and the PDF $H_N(t)$. For this purpose, we introduce a time cutoff $t_{\max}$ to be tenfold larger than either of the timescales $C = x_0^2/(4D)$ and b, discretize the time interval $[0, t_{\max}]$ with a small time step δ, and compute $S_\psi(t)$ at times $n\delta$ (with $n = 1, 2, \ldots, t_{\max}/\delta$) via a fast numerical convolution of the integral in Eq. (12). From the knowledge of $S_\psi(t)$, one can easily access both the PDF $H_N(t)$ and the mean fFPT $\langle \mathcal{T}_N \rangle$ via numerical integration in Eq. (15). Similarly, we evaluate numerically $\bar{S}_\psi(t)$ from Eq. (7) and thus access $\bar{H}_N(t)$ and $\langle \bar{\mathcal{T}}_N \rangle$. Varying both $t_{\max}$ and δ, we can control the accuracy of this numerical computation. In the following, we refer to the obtained PDF and the mean as "exact" results that will be compared to explicit but approximate asymptotic relations.

Let us first inspect the effect of an extended injection modeled by the gamma distribution (26), with $b = 1$ and three different values of ν. Figure 3(a) illustrates the PDF $H_\psi(t)$ of the delayed FPT $\tau_k + \delta_k$ for a single particle. As the profiles with larger ν delay the entrance, the corresponding PDFs are shifted to longer times. In turn, the limit $\nu \to 0$ formally corresponds to the instantaneous injection characterized by $H(t)$. One sees therefore how the extended injection modifies $H(t)$. The mean value is infinite, $\langle \tau_k + \delta_k \rangle = \infty$, while the most probable value grows with ν (note that $\langle \delta_k \rangle = \nu b$ and $T_{\mathrm{mp}} = (\nu - 1)b$). For comparison, we also show the PDF $\bar{H}_\psi(t)$ of the effective FPT $\bar{\tau}_k$. One sees that it is almost identical with $H_\psi(t)$ for the considered range of parameters and times. Figure 3(b) presents the corresponding survival probabilities $S_\psi(t)$ and $\bar{S}_\psi(t)$ for a single particle.

Figure 4 compares the mean fFPTs $\langle \mathcal{T}_N^0 \rangle$ and $\langle \mathcal{T}_N \rangle$ for instantaneous and extended injection of N particles modeled by the gamma distribution with $b = 1$ and $\nu = 5$. For the case of an instantaneous injection, the mean fFPT $\langle \mathcal{T}_N^0 \rangle$ is accurately approximated by the asymptotic relation (20), even for N as small as 100; moreover, the latter is close to the leading term
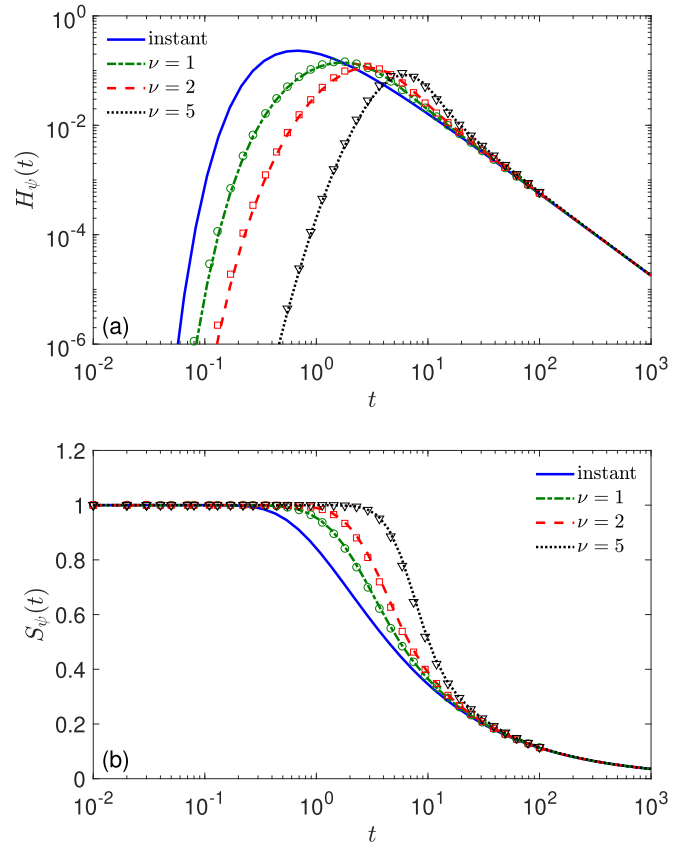

FIG. 3. (a) PDF $H_\psi(t)$ and (b) the survival probability $S_\psi(t)$ of the delayed FPT $\tau_k + \delta_k$ for diffusion on the half-line, with $x_0 = 2$, $D = 1$, and the injection profile given by the gamma model (26), with $b = 1$ and three values of ν. The solid line represents $H(t)$ and $S(t)$ of an instantaneous injection ($\nu = 0$). The symbols show $\bar{H}_\psi(t)$ and $\bar{S}_\psi(t)$ for the deterministic injection with the same set of parameters.

$C/\ln N$. The good quality of this asymptotic approximation for diffusion on the half-line was reported earlier in Ref. [12]. In contrast, the quality of this approximation is considerably worse for an extended injection with $\nu = 5$. On the one hand, we showed above that the survival probability $S_\psi(t)$ satisfies the asymptotic behavior (19) with $\bar{\mu} = 1$, allowing one to apply Lawley's asymptotic results. In particular, the asymptotic relation (20) holds with the unchanged leading order $C/\ln N$ and the correction term with modified parameters $\bar{\alpha} = \alpha + 2\nu$ and $\bar{A} = A(Cb)^{-\nu}$. One sees that this asymptotic relation indeed approaches the exact mean fFPT in the limit $N \to \infty$. On the other hand, the approach to this limiting behavior is extremely slow, and very large N are needed to get an accurate approximation (e.g., deviations are still noticeable even at $N = 10^{10}$).

Figure 5(a) presents the variance of the fFPT as a function of the overall number N of injected particles for the cases of instantaneous and extended-in-time injections. We observe that for an extended injection the variance is nearly two orders of magnitude larger than its counterpart for the instantaneous injection, meaning that the fFPT exhibits much stronger fluctuations in the former case than in the latter one. This emphasizes that, apparently, the knowledge of the mean fFPT alone is insufficient to gain a full understanding of the
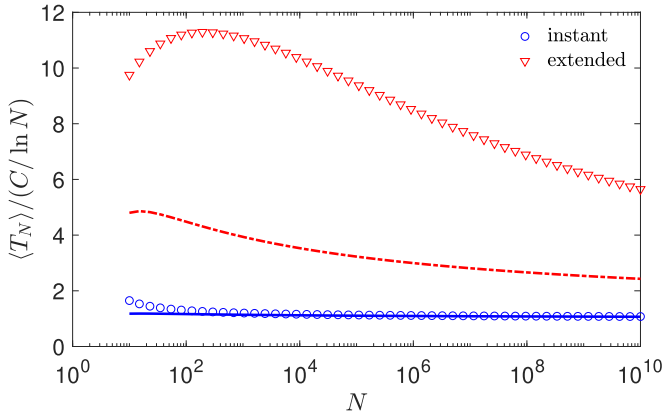
FIG. 4. Mean fFPTs $\langle \mathcal{T}_N^0 \rangle$ and $\langle \mathcal{T}_N \rangle$, rescaled by $C/\ln N$, as functions of N for diffusion on the half-line, with $x_0 = 2$, $D = 1$ (and thus $C = 1$ and $A = 1/\sqrt{\pi}$), for an instantaneous injection (circles) and an extended injection of N particles modeled by the gamma distribution (26) with $b = 1$ and $\nu = 5$ (triangles). The symbols show the mean fFPTs obtained by computing numerically the convolution in Eq. (12) and then evaluating the integral in Eq. (15), used as benchmarks. The lines present the asymptotic relation (20), with $\bar{\mu} = 1$, $\bar{C} = 1$, and two settings: $\bar{\alpha} = \alpha + 2\nu = 10.5$ and $\bar{A} = A(Cb)^{-\nu}$ for the extended injection (dashed line), and $\bar{\alpha} = \alpha = 0.5$ and $\bar{A} = A$ for the instantaneous injection (solid line). Overall, a considerable increase of the mean fFPT, by an order of magnitude, is observed for the case of the time-extended injection in this setting.

behavior in such a system and the analysis of the PDF is highly desirable. Figure 5(b) presents the coefficient of variation, defined as the ratio of the standard deviation of $\mathcal{T}_N$ and its mean value, $\sqrt{\mathrm{Var}\{\mathcal{T}_N\}}/\langle \mathcal{T}_N \rangle$. For the case of an extended injection, the coefficient of variation is somewhat larger than for the case of an instantaneous injection, but this difference is quite modest.

Figure 5(c) presents the variance, rescaled by its limiting behavior $V_N = \frac{\pi^2}{6} C^2/(\ln N)^4$ at very large N. For the case of instantaneous injection, this ratio is close to unity for both the exact variance and its asymptotic form (22), as expected. In turn, for the extended injection, the ratio $\mathrm{Var}\{\mathcal{T}_N\}/V_N$ exceeds unity significantly, by a factor of hundred, whereas the asymptotic relation (22) does not appear to work either. What is going wrong here? To answer this question, we recall that Eq. (22) relies on the large-x behavior of the Lambert function, $W_0(x) \approx \ln x - \ln(\ln x) + o(1)$ as $x \to \infty$. In this example, the argument of this function is $x = (N/\sqrt{\pi})^{1/10.5}/10.5 \leqslant 0.81$ for the whole considered range of N up to 10^{10}. In other words, even though the injection profile does not affect the leading-order behavior (i.e., $\bar{C} = C$), the change of α to $\bar{\alpha} = \alpha + 2\nu$ considerably reduces the range of applicability of the above asymptotic formulas. Moreover, the asymptotic formula (22), which represents only the leading term, is not accurate here because the subleading terms may provide significant contributions for the considered range of N. Even though the leading term becomes dominant in the limit $N \to \infty$, it is not sufficient for estimating the variance at intermediate values of N.

Figure 6 illustrates the PDF $H_N(t)$ of the fastest FPT $\mathcal{T}_N$ for an extended random injection modeled by the gamma
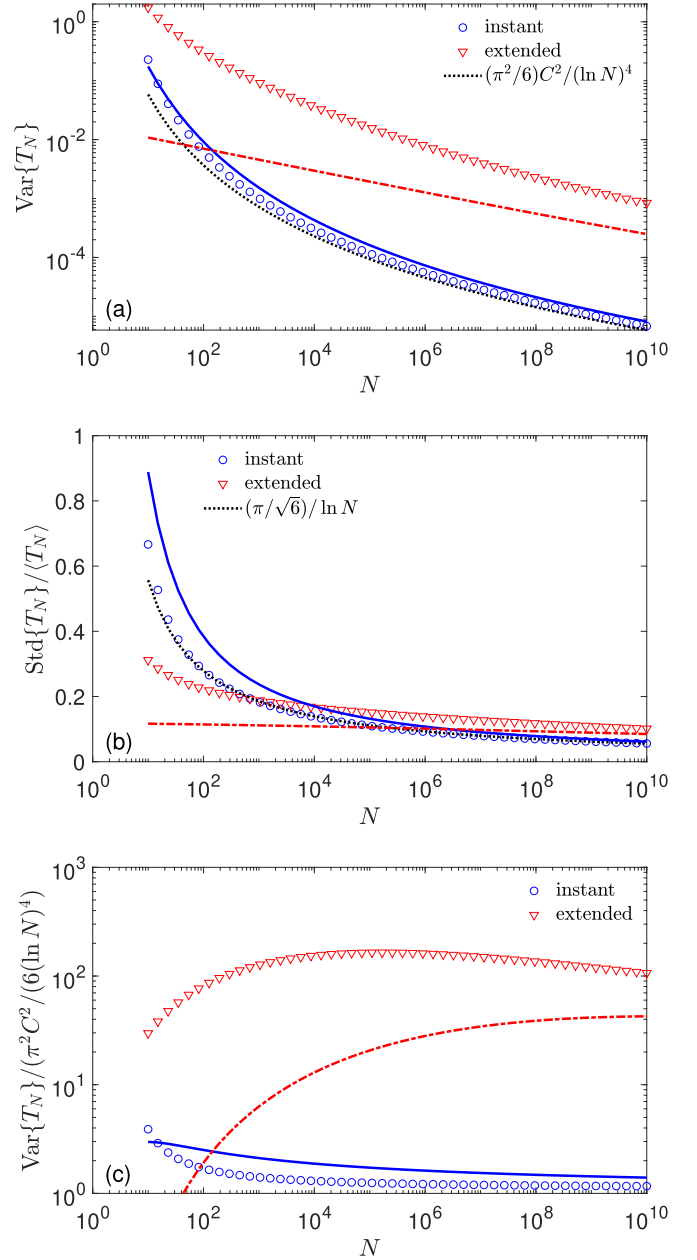

FIG. 5. (a) Variance of the fFPT $\mathcal{T}_N$ as a function of N for diffusion on the half-line, with $x_0 = 2$, $D = 1$ (and thus $C = 1$ and $A = 1/\sqrt{\pi}$), with an extended injection of N particles modeled by the gamma distribution (26) with $b = 1$ and $\nu = 5$. For comparison, the variance of the fFPT $\mathcal{T}_N^0$ for an instantaneous injection is shown. The symbols show the exact variance, obtained from computing numerically the convolution in Eq. (12) and then by evaluating the first and second moments of $\mathcal{T}_N$ via the integrals $\int_0^\infty dt \, [S_\psi(t)]^N$ and $2\int_0^\infty dt \, t [S_\psi(t)]^N$. The solid and dashed lines present Lawley's asymptotic relation (C7), in which a_N is given by Eq. (C2), either with parameters C, α, and A for the instantaneous injection (solid line), or with parameters $\bar{C} = C$, $\bar{\alpha} = \alpha + 2\nu$, and $\bar{A} = A(Cb)^{-\nu}$ for extended injection (dashed line). Note that the black dotted line indicates the lowest-order behavior $V_N = \frac{\pi^2}{6} C^2/(\ln N)^4$. (b) The coefficient of variation, $\sqrt{\mathrm{Var}\{\mathcal{T}_N\}}/\langle \mathcal{T}_N \rangle$, for the same two settings of instantaneous and extended injections, with the black dotted line indicating the lowest-order behavior. (c) The variance rescaled by its leading-order term V_N given by Eq. (24).
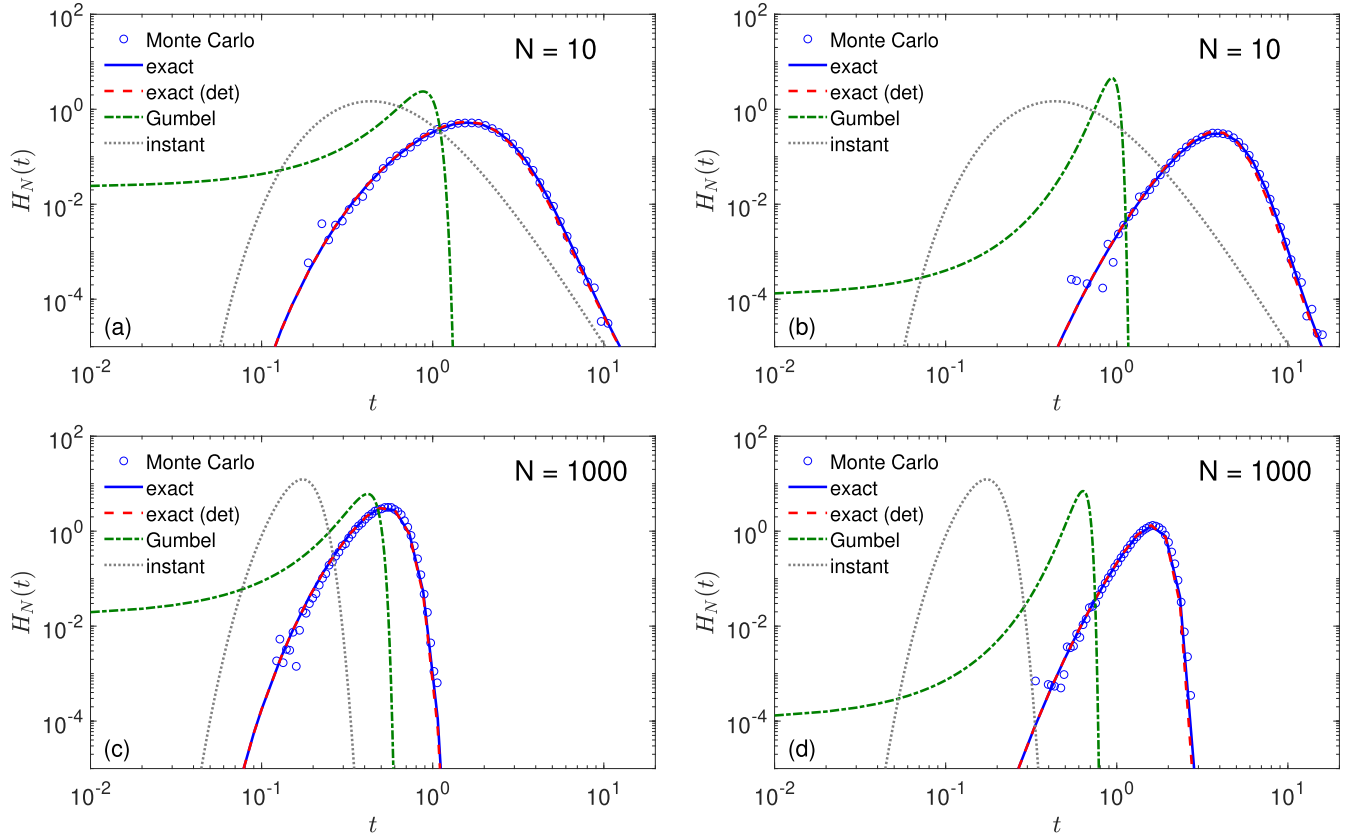
FIG. 6. PDF $H_N(t)$ of the fastest FPT $\mathcal{T}_N$ for diffusion on the half-line, with $x_0 = 2$, $D = 1$ (and thus $C = 1$), and an extended injection modeled by the gamma distribution (26) with $b = 1$, and four combinations of ν and N: (a) $\nu = 2$, $N = 10$; (b) $\nu = 5$, $N = 10$; (c) $\nu = 2$, $N = 1000$, and (d) $\nu = 5$, $N = 1000$. The circles represent rescaled histograms obtained by generating $\mathcal{T}_N$ (with 10^5 realizations). The solid line represents the exact solution $H_N(t) = N H_\psi(t) [S_\psi(t)]^{N-1}$, where $H_\psi(t)$ and $S_\psi(t)$ are obtained via fast numerical convolutions. The dashed line shows the exact solution $\bar{H}_N(t) = N \bar{H}_\psi(t) [\bar{S}_\psi(t)]^{N-1}$, where $\bar{H}_\psi(t)$ and $\bar{S}_\psi(t)$ are obtained via fast numerical convolutions. The dash-dotted line represents the asymptotic Gumbel distribution, with the scale and location parameters a_N and b_N given by Eq. (C2) with the modified parameters $\bar{A} = aAC^{-\nu}\Gamma(\nu)$ and $\bar{\alpha} = \alpha + 2\nu$; see Appendix B. The dotted line indicates the exact distribution for an instantaneous injection.

distribution (26) with $b = 1$ and two values of the scale parameter: $\nu = 2$ and $\nu = 5$. In agreement with the above analysis, the PDF is shifted to the left (to shorter times) and narrows with increasing N. The exact solution determined from $H_\psi(t)$ and $S_\psi(t)$ shows excellent agreement with Monte Carlo simulations. Moreover, the PDF $\bar{H}_N(t)$ of $\bar{\mathcal{T}}_N$ for the deterministic injection with the same profile is almost indistinguishable from $H_N(t)$, demonstrating the asymptotic equivalence between $\mathcal{T}_N$ and $\bar{\mathcal{T}}_N$ even for moderate N. This figure highlights two important conclusions:

(i) First, an extended injection of particles substantially delays the arrival of the fastest particle; in particular, the typical time of the first arrival that characterizes the maximum of the PDF, is shifted to longer times as compared to the instantaneous injection of the same number of particles. For instance, in the case $\nu = 5$ and the considered values of N, a tenfold delay is observed. This delay is weaker for $\nu = 2$ but it can be much more substantial for larger ν, i.e., for a faster decay of $\psi(t)$. As a consequence, neglecting an extended injection, as done in former works on this topic, may lead to strong misrepresentations.

(ii) Second, the Gumbel distribution as a universal large-N limit of the fastest FPT may also yield inaccurate predictions

when applied to biologically relevant amounts of diffusing particles. As N increases, the right tail of the Gumbel distribution becomes increasingly accurate, but an extremely large N is needed for its applicability for extended injection. In other words, there exists an intermediate range of N, for which the Gumbel distribution is not applicable. This limitation originates from an extended injection because the Gumbel distribution was seen to be quite accurate even for moderate N in the case of an instantaneous injection (see Fig. 7 in Appendix C). This is consistent with the above analysis of the mean fFPT, for which the asymptotic formulas were also much more accurate for the case of instantaneous injection. Finding an appropriate approximation for the PDF $H_N(t)$ at intermediate values of N presents an interesting open problem.

V. DISCUSSION

A. Approach to the Gumbel distribution

The distribution of the minimum of a large number N of independent random variables is known to approach a Gumbel distribution as $N \to \infty$. In our setting of the fFPT, it means

that

$$H_N(t) \underset{N \to \infty}{\sim} \frac{H^{\mathrm{G}}\left(\frac{t-b_N}{a_N}\right)}{a_N}, \quad H^{\mathrm{G}}(x) = \exp(x - e^x), \quad (27)$$

with appropriate scale and location parameters a_N and b_N [note that $\exp(-x - e^{-x})$ that is often referred to as the Gumbel density, corresponds to $H^{\mathrm{G}}(-x)$]. For the case of an instantaneous injection of N particles, Lawley found the asymptotic behavior of these two parameters under the assumption (17) on the short-time behavior of the survival probability $S(t)$ (see [12] and a summary in Appendix C). Despite the universal character of this law, an approach of $H_N(t)$ to its limiting Gumbel form as N becomes large can be extremely slow. In this light, it is remarkable how accurately the Gumbel density H^{G} does approximate $H_N(t)$ even for moderately large N in earlier-studied examples of the diffusive dynamics under an instantaneous injection (see examples in Ref. [12], as well as Fig. 7 in Appendix C). Conversely, our numerical results from Sec. III D illustrate the opposite—and presumably more generic—situation of a very slow convergence. Indeed, even though the injection profile with a power-law behavior at short times does not change the leading-order terms of a_N and b_N, the Gumbel distribution does not approximate $H_N(t)$ for moderately large N, as shown in Fig. 6. Moreover, the asymptotic behavior of $H_N(t)$ turns out to be quite sensitive to the preexponential (subleading) factor and its exponent $\bar{\alpha} = \alpha + 2\nu$. In particular, a faster power-law decay of the injection profile $\psi(t)$ as $t \to 0$ effects larger deviations from the Gumbel distribution. However, it is instructive to mention that this empirical observation is not valid in general. To illustrate this point, let us consider an injection profile of the form

$$\psi(t) = \frac{\sqrt{c}\, e^{-c/t}}{\sqrt{\pi t^3}}, \quad (28)$$

with the timescale $c > 0$. As this profile vanishes faster than any power-law as $t \to 0$, one might intuitively expect that the convergence would be even worse for this profile. However, it is easy to check that Eq. (13) yields

$$H_\psi(t) = \frac{\sqrt{c} + \sqrt{C}}{\sqrt{\pi t^3}} \exp\left(-\frac{[\sqrt{c} + \sqrt{C}]^2}{t}\right), \quad (29)$$

where $C = x_0^2/(4D)$, i.e., we get exactly the same probability density as for an instantaneous injection, only with the rescaled parameter $\bar{C} = (\sqrt{c} + \sqrt{C})^2$ instead of C. As a consequence, the approach of $H_N(t)$ to the Gumbel density should be as rapid as for the instantaneous injection. In summary, the convergence rate to the Gumbel distribution, as well as the approximate forms of $H_N(t)$ for moderately large N need to be better understood.

B. Random injection

In the case of random injection, it may be informative to perform the asymptotic analysis of the survival probability $S_\psi(t)$ in the Laplace domain. In fact, the short-time behavior of $S_\psi(t)$ can be determined from the large-p behavior of its

Laplace transform,

$$\tilde{S}_\psi(p) = \int_0^\infty dt\, e^{-pt}\, S_\psi(t) = \frac{1 - \tilde{H}_\psi(p)}{p}, \quad (30)$$

where

$$\tilde{H}_\psi(p) = \int_0^\infty dt\, e^{-pt} H_\psi(t) = \langle e^{-p(\tau_k + \delta_k)} \rangle = \tilde{H}(p)\tilde{\psi}(p), \quad (31)$$

due to the independence of τ_k and δ_k. To proceed, it is convenient to reformulate the condition (17) in the Laplace domain. Using the identity

$$\int_0^\infty dz\, z^{\nu-1} e^{-c/z - z/b} = 2(cb)^{\nu/2} K_\nu(2\sqrt{c/b}), \quad (32)$$

where $K_\nu(z)$ is the modified Bessel function of the second kind, we can evaluate the Laplace transform of Eq. (17) as

$$\frac{1}{p} - \tilde{S}(p) \sim 2A(C/p)^{(\alpha+1)/2} K_{\alpha+1}(2\sqrt{Cp})$$
$$\approx \sqrt{\pi} A C^{\alpha/2+1/4} p^{-\alpha/2-3/4} e^{-2\sqrt{Cp}} \quad (p \to \infty), \quad (33)$$

where we used the asymptotic behavior of the modified Bessel function at large argument. In other words, one can use either the condition (17) in the time domain or the condition (33) in the Laplace domain. Note that Eq. (33) can also be written as

$$\tilde{H}(p) \sim \sqrt{\pi} A C^{\alpha/2+1/4} p^{-\alpha/2+1/4} e^{-2\sqrt{Cp}} \quad (p \to \infty). \quad (34)$$

In this way, one can further analyze the effect of the injection profile $\psi(t)$ through the large-p asymptotic behavior of its Laplace transform $\tilde{\psi}(p)$.

C. On the short-time limit

We emphasize the following points. In the present paper, as well as in the previous works on the instantaneous injection of N particles into the domain of interest [8,10–18], it is stipulated that the particles perform a standard Brownian motion from time $t = 0$. That implies that there is a tacit underlying assumption that each particle, during an infinitesimally small time interval $\delta t \to 0$ moves an infinitesimally small distance $\delta a \to 0$, with the ratio $D = \delta a^2/(2\delta t)$ kept fixed. Such an assumption is conventional and valid for many practically important situations. Concurrently, as it was demonstrated here as well as in the previous works, in the limit $N \to \infty$ the corresponding asymptotic forms of the survival probability and the ensuing fFPT-PDF become fully dominated by the behavior of the process in a very short time span in the vicinity of $t = 0$. In the limit $N \to \infty$, this span becomes so small that a particle can make, at most, a few jumps away from its initial location, and its short-time dynamics in realistic systems may be very different from that of a conventional (continuous) Brownian motion. Indeed, for the latter a particle may travel on any distance within an arbitrarily short time interval with an exponentially small but nonzero probability, while in realistic settings this probability should be identically equal to

zero up to a certain time instant.[1] This signifies, in particular, that the logarithmic reduction of the mean first-passage time in Eq. (16), as well as our results presented here are only valid for sufficiently large but still *bounded* values of N, such that the time-interval which dominates the behavior of the survival probability should remain sufficiently large permitting to use the Brownian motion picture.

The true asymptotic behavior of the characteristic properties in the mathematical limit $N \to \infty$ may appear somewhat different, but to determine it one would need to start with a discrete-space approach which captures the small nuances of the short-time behavior, especially in the case of processes with a broad distribution of waiting times, which ultimately results in a large-scale subdiffusive motion. Such a robust approach is lacking at present but clearly represents a challenging and pressing issue.

VI. CONCLUSIONS

In summary, we investigated the effect of an extended, time-dependent injection (or entrance) of particles on the statistics of the fastest arrival $\mathcal{T}_N$ to the target. While a formal implementation of prescribed time delays δ_k is straightforward for independently diffusing particles, the asymptotic analysis of the PDF $H_N(t)$ of the fastest FPT $\mathcal{T}_N$ and its mean $\langle \mathcal{T}_N \rangle$ at large N required a substantial reformulation of the problem. The first deterministic formulation was based on a smooth approximation of the injection profile $\psi(t)$ and allowed us to introduce effective first-passage times $\bar{\tau}_k$ that account for a given profile through the modified survival probability $\bar{S}_\psi(t)$ given by Eq. (7). The second probabilistic formulation treated the delay times δ_k as independent random variables generated from the profile $\psi(t)$ so that the delayed FPTs $\tau_k + \delta_k$ were determined by the survival probability $S_\psi(t)$ given by Eq. (12). We showed that both formulations yielded remarkably similar results, even for a single particle (see Fig. 3).

Next, we analyzed the impact of the injection profile $\psi(t)$ onto the survival probability $S_\psi(t)$. Under rather general assumptions on the short-time behaviors of $S(t)$ and $\psi(t)$, we derived the short-time behavior of $S_\psi(t)$ and thus the large-N asymptotic behavior (20) of the mean fFPT. This is an extension of former results known for an instantaneous injection. We also showed that the extended injection considerably slows down the approach of the mean fFPT to its asymptotic value in the limit $N \to \infty$. Similarly, we showed that an approach of $H_N(t)$ to its limiting Gumbel distribution upon an increase of N is also very slow, such that the Gumbel distribution may not be applicable for an intermediate range of N from tens to thousands, which is the most relevant scenario in molecular biology. This result urges for further investigations of this fundamental problem and obtaining correction terms to the Gumbel distribution in this setting.

DATA AVAILABILITY

No data were created or analyzed in this study.

APPENDIX A: SURVIVAL PROBABILITY $\bar{S}_\psi(t)$

In this Appendix, we discuss some properties of the survival probability $\bar{S}_\psi(t)$ defined by Eq. (7). We here assume that the survival probability $S(t)$ vanishes as $t \to \infty$ (as it is always the case for diffusion in a bounded domain) and aim at showing that $\bar{S}_\psi(t)$ monotonously decreases to 0 as t increases. For convenience, we introduce the notation

$$f_\psi(t) = -\int_0^t dt' \, \psi(t') \ln S(t - t'). \tag{A1}$$

First, Jensen's inequality for the concave function $\ln(z)$ implies

$$\frac{1}{1 - \Psi(t)} \int_0^t dt' \, \psi(t') \ln S(t - t')$$

$$\leqslant \ln\left(\frac{1}{1 - \Psi(t)} \int_0^t dt' \, \psi(t') \, S(t - t')\right), \tag{A2}$$

where

$$\Psi(t) = \int_t^\infty dt' \, \psi(t'). \tag{A3}$$

Second, the integral on the right-hand side can be split into the two contributions

$$I(t) = \int_0^t dt' \, \psi(t') \, S(t - t')$$

$$= \int_0^{t/2} dt' \, \psi(t') \, S(t - t') + \int_0^{t/2} dt' \, \psi(t - t') \, S(t'), \tag{A4}$$

where the integration variable t' was changed to $t - t'$ in the second integral. As the survival probability $S(t)$ is a monotonously decreasing function, one can estimate the first integral as

$$\int_0^{t/2} dt' \, \psi(t') \, S(t - t') \leqslant S(t/2) \int_0^{t/2} dt' \, \psi(t') \leqslant S(t/2), \tag{A5}$$

where the last integral was extended to $+\infty$ and then replaced by unity due to the normalization of $\psi(t)$. Since $S(t)$ vanishes in the limit $t \to \infty$, this contribution vanishes. Similarly, we estimate the second integral as

$$\int_0^{t/2} dt' \, \psi(t - t') \, S(t')$$

$$\leqslant \int_0^{t/2} dt' \, \psi(t - t') = \Psi(t/2) - \Psi(t). \tag{A6}$$

---

[1]Such a finite-horizon behavior is, e.g., essential in the description of heat conduction dynamics, for which the diffusion equation is typically replaced by the hyperbolic telegrapher's or Cattaneo equation, endowing the process with a finite propagation speed [37,38].

In the long-time limit, $\Psi(t)$ vanishes and thus does the second integral. We conclude that $I(t) \to 0$ as $t \to \infty$ so that the right-hand side of Eq. (A2) goes to $-\infty$ and thus $f_\psi(t)$ from Eq. (A1) diverges to $+\infty$, whereas $\bar{S}_\psi(t) = e^{-f_\psi(t)}$ vanishes.

Note that the inequality (A2) also implies that

$$\bar{S}_\psi(t) \leqslant \exp\left((1 - \Psi(t)) \ln \left(\frac{\int_0^t dt'\, \psi(t')\, S(t-t')}{1 - \Psi(t)} \right) \right)$$

$$= \left(1 - \frac{1 - S_\psi(t)}{1 - \Psi(t)} \right)^{1 - \Psi(t)}, \tag{A7}$$

where we used the definition (12) of $S_\psi(t)$. Note that Eq. (12) implies that $S_\psi(t) \geqslant \Psi(t)$, i.e., the right-hand side is nonnegative. Re-arranging the above inequality, one gets the equivalent form

$$S_\psi(t) \geqslant \Psi(t) + (1 - \Psi(t))[\bar{S}_\psi(t)]^{1/(1 - \Psi(t))}. \tag{A8}$$

Since $(1 - x/a)^a \leqslant 1 - x$ for any $x \in (0, a)$ and any $0 < a \leqslant 1$, one can also deduce from the inequality (A7) the simpler bound

$$\bar{S}_\psi(t) \leqslant S_\psi(t). \tag{A9}$$

The probabilistic interpretation of this inequality is that the first-passage time $\bar{\tau}_k$ is typically smaller than $\tau_k + \delta_k$, i.e., the deterministic injection is faster than the random one [for the same profile $\psi(t)$].

APPENDIX B: SHORT-TIME BEHAVIOR OF THE SURVIVAL PROBABILITY

In this Appendix, we derive the short-time asymptotic behavior of the survival probabilities $S_\psi(t)$ and $\bar{S}_\psi(t)$.

Rewriting Eq. (12) as

$$1 - S_\psi(t) = \int_0^t dt'\, \psi(t - t')(1 - S(t')) \tag{B1}$$

and substituting the asymptotic relations (17) and (18), we get

$$1 - S_\psi(t) \approx \int_0^t dt'\, a(t - t')^{\nu - 1} e^{-c^\mu/(t-t')^\mu} A(t')^\alpha e^{-C/t'}$$

$$= aA t^{\nu + \alpha} \int_0^1 dz\, z^\alpha (1 - z)^{\nu - 1}$$

$$\times e^{-(c/t)^\mu (1-z)^{-\mu} - (C/t)/z}, \tag{B2}$$

where we changed the integration variable to $t' = tz$. To estimate the asymptotic behavior of this integral in the limit $t \to 0$, we write the exponential function as $e^{-(c/t)^\mu f(z)}$, with

$$f(z) = \frac{1}{(1 - z)^\mu} + \frac{\mu B}{z}, \quad B = \frac{C t^{\mu - 1}}{\mu c^\mu} \tag{B3}$$

and apply the Laplace method. For this purpose, one determines z_0 as the minimum of the function $f(z)$, given by the equation

$$f'(z_0) = \frac{\mu}{(1 - z_0)^{\mu+1}} - \frac{\mu B}{z_0^2} = 0. \tag{B4}$$

As a consequence, the integral reads

$$1 - S_\psi(t) \approx aA t^{\nu + \alpha} e^{-(c/t)^\mu f(z_0)} z_0^\alpha (1 - z_0)^{\nu - 1}$$

$$\times \sqrt{\frac{2\pi t^\mu}{c^\mu f''(z_0)}}. \tag{B5}$$

We consider the following four cases:

(i) For $\mu > 1$, the factor $(c/t)^\mu$ is dominant. At very short times t, one has $B \ll 1$, so that z_0 is small and the above equation can be solved as $z_0 \approx \sqrt{B} \ll 1$, and thus $f(z_0) \approx 1 + 2\mu\sqrt{B}$ and $f''(z_0) \approx \mu(\mu + 1) + 2\mu/\sqrt{B}$. To leading order, we get

$$1 - S_\psi(t) \approx aA t^{\nu + \mu(2\alpha+3)/4 - 1/4} e^{-(c/t)^\mu}$$

$$\times (C/(\mu c^\mu))^{\alpha/2 + 1/4} \sqrt{\frac{\pi}{c^\mu \mu}}. \tag{B6}$$

We therefore find the asymptotic behavior (19) with

$$\bar{C} = c, \quad \bar{\mu} = \mu, \tag{B7a}$$

$$\bar{\alpha} = \nu + \mu(2\alpha + 3)/4 - 1/4, \tag{B7b}$$

$$\bar{A} = aA(C/(\mu c^\mu))^{\alpha/2 + 3/4}\sqrt{\pi/C}. \tag{B7c}$$

(ii) For $\mu = 1$, one can solve Eq. (B4) to get $z_0 = \sqrt{B}/(1 + \sqrt{B})$, where $B = C/c$ is independent of t. One then finds $f(z_0) = (1 + \sqrt{B})^2$ and $f''(z_0) = 2(1 + 1/\sqrt{B})$, from which

$$1 - S_\psi(t) \approx aA t^{\nu + \alpha + 1/2} e^{-(\sqrt{c} + \sqrt{C})^2/t}$$

$$\times \frac{B^{\alpha/2 + 1/4}}{(1 + \sqrt{B})^{\alpha + \nu + 1/2}} \sqrt{\pi/c}. \tag{B8}$$

In other words, we retrieve the asymptotic behavior (19) with the parameters

$$\bar{C} = \left(\sqrt{c} + \sqrt{C} \right)^2, \quad \bar{\mu} = 1, \tag{B9a}$$

$$\bar{\alpha} = \alpha + \nu + 1/2, \tag{B9b}$$

$$\bar{A} = aA \frac{(C/c)^{\alpha/2 + 1/4}}{(1 + \sqrt{C/c})^{\alpha + \nu + 1/2}} \sqrt{\pi/c}. \tag{B9c}$$

(iii) For $0 < \mu < 1$, one has $B \gg 1$ in the short-time limit, so that the solution of Eq. (B4) is approximately $z_0 \approx 1 - B^{-1/(1+\mu)}$ and thus $f(z_0) \approx t^{\mu - 1} C/c^\mu$ and $f''(z_0) = \mu(\mu + 1)B^{(\mu+2)/(\mu+1)} + 2\mu B$, such that

$$1 - S_\psi(t) \approx aA t^{\alpha + (2\nu + \mu)/(\mu+1)} e^{-C/t}$$

$$\times (C/(\mu c^\mu))^{-(\nu + \mu/2)/(\mu+1)} \sqrt{\frac{2\pi}{c^\mu \mu(\mu+1)}}. \tag{B10}$$

Once again, we find Eq. (19), with

$$\bar{C} = C, \quad \bar{\mu} = 1, \tag{B11a}$$

$$\bar{\alpha} = \alpha + (2\nu + \mu)/(\mu + 1), \tag{B11b}$$

$$\bar{A} = aA(C/(\mu c^\mu))^{-(\nu + \mu/2)/(\mu+1)} \sqrt{\frac{2\pi}{c^\mu \mu(\mu+1)}}. \tag{B11c}$$

(iv) The case $\mu = 0$ requires a separate analysis because Eq. (B11c) either vanishes or diverges as $\mu \to 0$. Here one has to distinguish the cases $\nu > 1$ and $\nu \leqslant 1$. We discuss only

the former case when the injection profile vanishes at $t = 0$, for which

$$1 - S_\psi(t) \approx aAt^{\alpha+\nu} \int_0^1 dz \, \exp(-f(z)), \qquad (B12)$$

with $f(z) = C/(tz) - \alpha \ln z - (\nu - 1)\ln(1 - z)$. The minimum z_0 of this function via

$$f'(z_0) = -\frac{C}{tz_0^2} - \frac{\alpha}{z_0} + \frac{\nu - 1}{1 - z_0} = 0. \qquad (B13)$$

As C/t is large, the first term should be compensated by the third term, such that z_0 should be close to 1. Substituting $z_0 = 1 - \varepsilon$ into this equation and expanding up to linear order in ε, we get $\varepsilon \approx (\nu - 1)/(C/t + \alpha + 2(\nu - 1))$. To leading order, we also get

$$f''(z_0) = \frac{2C}{tz_0^3} + \frac{\alpha}{z_0^2} + \frac{\nu - 1}{(1 - z_0)^2} \approx \frac{(t/C)^2}{\nu - 1}. \qquad (B14)$$

The Laplace method yields again Eq. (19) to leading order, with

$$\bar{C} = C, \quad \bar{\mu} = 1, \qquad (B15a)$$

$$\bar{\alpha} = \alpha + 2\nu, \qquad (B15b)$$

$$\bar{A} = aAC^{-\nu} \left[e^{1-\nu}(\nu - 1)^\nu \sqrt{2\pi/(\nu - 1)} \right] \qquad (B15c)$$

$$\approx aAC^{-\nu}\Gamma(\nu). \qquad (B15d)$$

For the last relation, we identified the factor in the square brackets as the Stirling expansion of the gamma function $\Gamma(\nu)$ for $\nu \gg 1$. Note that the above estimation gets more accurate for large ν.

While we focused on the analysis of the survival probability $S_\psi(t)$, the above results are also applicable to $\bar{S}_\psi(t)$. In fact, one has

$$1 - \bar{S}_\psi(t) = 1 - \exp\left(\int_0^t dt' \, \psi(t - t') \ln(1 - (1 - S(t'))) \right)$$

$$\approx \int_0^t dt' \, \psi(t - t')(1 - S(t'))$$

$$= 1 - S_\psi(t) \quad (t \to 0), \qquad (B16)$$

where the logarithm was expanded into a Taylor series in powers of $(1 - S(t'))$, which is small at short times. Note that the correction term includes $(1 - S_\psi(t))^2$ and an integral involving $(1 - S(t'))^2$, which are both exponentially small as compared to $1 - S_\psi(t)$.

APPENDIX C: PRIMER ON THE ASYMPTOTIC RESULTS FOR INSTANTANEOUS INJECTION

In the large N limit, the fastest FPT $\mathcal{T}_N^0 = \min\{\tau_1, \ldots, \tau_N\}$ for the case of instantaneous injection converges to the Gumbel distribution with the scale and location parameters a_N and b_N, i.e., $(\mathcal{T}_N^0 - b_N)/a_N$ converges in distribution to a random variable X obeying the standard Gumbel distribution $\mathbb{P}\{X > x\} = \exp(-e^x)$ on $\mathbb{R}$. Under the assumption (17) on the short-time behavior of the survival probability $S(t)$, Lawley derived two equivalent asymptotic forms for the

parameters a_N and b_N [12]. The first form is more accurate but less explicit,

$$a_N = \frac{b_N}{\ln(AN)}, \quad b_N = \frac{C}{\ln(AN)} \quad (\alpha = 0), \qquad (C1)$$

$$a_N = \frac{b_N}{\alpha(1 + W)}, \quad b_N = \frac{C}{\alpha W} \quad (\alpha \neq 0), \qquad (C2)$$

and

$$W = \begin{cases} W_0(C(AN)^{1/\alpha}/\alpha) & (\alpha > 0), \\ W_{-1}(C(AN)^{1/\alpha}/\alpha) & (\alpha < 0), \end{cases} \qquad (C3)$$

where $W_0(z)$ denotes the principal branch of the Lambert W-function and $W_{-1}(z)$ denotes the lower branch [39]. The second form (denoted by a prime) can be deduced from the asymptotic behavior of the Lambert function [12],

$$a_N' = \frac{C}{(\ln N)^2}, \quad b_N' = \frac{C}{\ln N} + \frac{C[\alpha \ln \ln N - \ln(AC^\alpha)]}{(\ln N)^2}. \qquad (C4)$$

In particular, the mean and variance of $\mathcal{T}_N^0$ (whenever they exist) are

$$\langle \mathcal{T}_N^0 \rangle \approx b_N - a_N\gamma + o(a_N), \qquad (C5)$$

$$\approx \frac{C}{\ln N} + C\frac{\alpha \ln \ln N - \ln(AC^\alpha) - \gamma}{(\ln N)^2} \qquad (C6)$$

and

$$\text{Var}\{\mathcal{T}_N^0\} \approx \frac{\pi^2}{6}a_N^2 + o(a_N^2) \qquad (C7)$$

$$\approx \frac{\pi^2}{6}\frac{C^2}{(\ln N)^4}, \qquad (C8)$$

where $\gamma \approx 0.5772$ is the Euler constant. Note also that the most probable time of the Gumbel distribution is precisely given by b_N, i.e.,

$$\mathcal{T}_{N,\text{mp}}^0 = b_N \approx \frac{C}{\ln N} + O(1/(\ln N)^2). \qquad (C9)$$

Figure 7 shows the PDF $H_N(t)$ for an instantaneous injection of N particles diffusing in the half-line. One sees how the distribution slowly approaches the asymptotic Gumbel distribution. We recall that both the mean fFPT $\langle \mathcal{T}_N^0 \rangle \simeq C/\ln(N)$ and the coefficient of variation, $\text{Std}\{\mathcal{T}_N^0\}/\langle \mathcal{T}_N^0 \rangle \simeq (\pi/\sqrt{6})/\ln(N)$, slowly decrease with N. As a consequence, the PDF shifts to the left (to shorter times) and gets narrower as N increases. Note also that the typical value decreases, as well.

APPENDIX D: UNIFORM ENTRANCE TIMES

We here briefly discuss another common setting when the entrance times δ_k are uniformly distributed over a time span from 0 to T. This injection profile,

$$\psi(t) = \frac{\Theta(T - t)}{T}, \qquad (D1)$$

in Laplace domain yields $\tilde{\psi}(p) = (1 - e^{-pT})/(pT)$, that allows one to evaluate the survival probability $S_\psi(t)$ explicitly
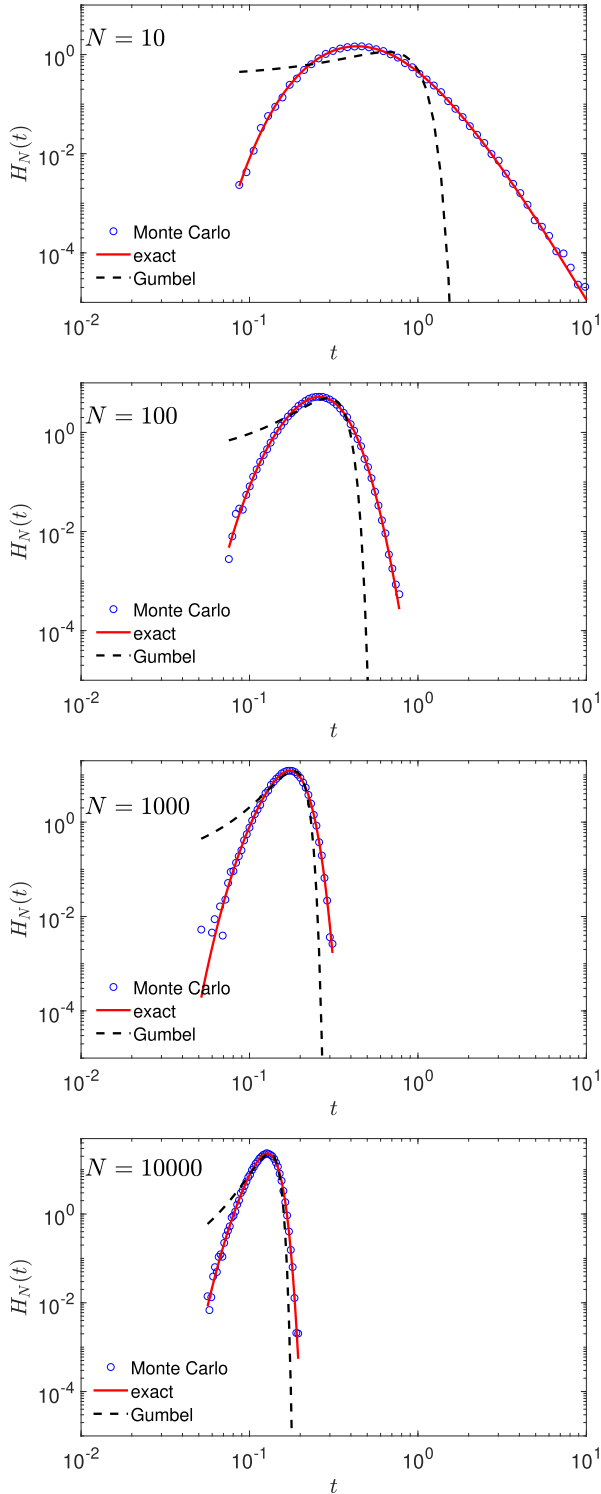
FIG. 7. PDF $H_N^0(t)$ of the fastest FPT $\mathcal{T}_N^0$ for diffusion on the half-line, with $x_0 = 2$, $D = 1$, and an instantaneous injection of N particles, for four values of N (from top to bottom): $N = 10$, $N = 100$, $N = 1000$, and $N = 10\,000$. The circles represent rescaled histograms obtained by generating $\mathcal{T}_N^0$ (with 10^5 realizations); the solid line gives the exact solution $H_N^0(t) = NH(t)[S(t)]^{N-1}$; the dashed line shows the asymptotic Gumbel distribution, with the parameters a_N and b_N given by Eq. (C2) derived by Lawley [12].

in the case of diffusion on the half-axis, namely,

$$S_\psi(t) = 1 - \frac{t}{T}F(x_0/\sqrt{4Dt})$$
$$- \frac{t - T}{T}\Theta(t - T)F(x_0/\sqrt{4D(t - T)}), \quad \text{(D2)}$$

where

$$F(z) = (1 + 2z^2)\text{erfc}(z) - \frac{2}{\sqrt{\pi}}ze^{-z^2}. \quad \text{(D3)}$$

At short times, the last term in Eq. (D2) is zero due to the Heaviside step function. In turn, the second term can be simplified by using $F(z) \approx e^{-z^2}/(\sqrt{\pi}z^3)$ as $z = x_0/\sqrt{4Dt} \to \infty$, so that we retrieve the asymptotic behavior (19), with

$$\bar{\mu} = \mu = 1, \quad \bar{C} = C = \frac{x_0^2}{4D}, \quad \bar{\alpha} = \frac{5}{2}, \quad \bar{A} = \frac{1}{\sqrt{\pi}\,T\,C^{3/2}}. \quad \text{(D4)}$$

As the uniform profile (D1) exhibits the short-time asymptotic behavior (18) with $\nu = 1$ and $\mu = 0$, the parameters $\bar{\alpha}$ and $\bar{A}$ agree with our general expressions (B15). Note also that

$$H_\psi(t) = \frac{1}{T}\text{erfc}(x_0/\sqrt{4Dt})$$
$$- \frac{\Theta(t - T)}{T}\text{erfc}(x_0/\sqrt{4D(t - T)}). \quad \text{(D5)}$$

Figure 8 illustrates the main features of the fFPT $\mathcal{T}_N$ for the uniform injection profile: Figs. 8(a) and 8(b) present the PDF $H_N(t)$ for $T = 10$, whereas Fig. 8(c) shows the mean fFPT as a function of N for $T = 1$ and $T = 10$. It is instructive to compare these results to those presented in the main text for the injection modeled by a gamma distribution. For a proper comparison, we impose that the mean delay time, $\langle\delta_k\rangle$, is the same in both cases—under this condition, the uniform distribution with $T = 10$ can be compared to the gamma distribution with $b = 1$ and $\nu = 5$. Qualitatively, the PDFs for both cases look similar [compare Figs. 8(a), 8(b) with Figs. 6(b), 6(d)], but the density $H_N(t)$ is shifted to longer times for the gamma profile. This is consistent with the observation that the mean fFPT (shown in Fig. 4) is longer for the gamma profile, and it approaches slower to the leading-order term $C/\ln N$. We emphasize that the leading-order term $C/\ln N$ is the same for both injection profiles such that the actual shape of the profile influences only the sub-leading term in Eq. (20), as well as the accuracy of this asymptotic relation.

Figure 8(c) also highlights that the longer mean delay time $\langle\delta_k\rangle$ (here, $T/2$), expectedly, increases the mean fFPT $\langle\mathcal{T}_N\rangle$, but its effect strongly depends on the number N of particles. Moreover, it is in general difficult to distinguish the relative roles of the mean delay time and the shape of its distribution, as both affect the subleading term in Eq. (20) via the modified parameters $\bar{\alpha}$ and $\bar{A}$. Our theoretical description allows one to analyze these effects for various injection profiles.
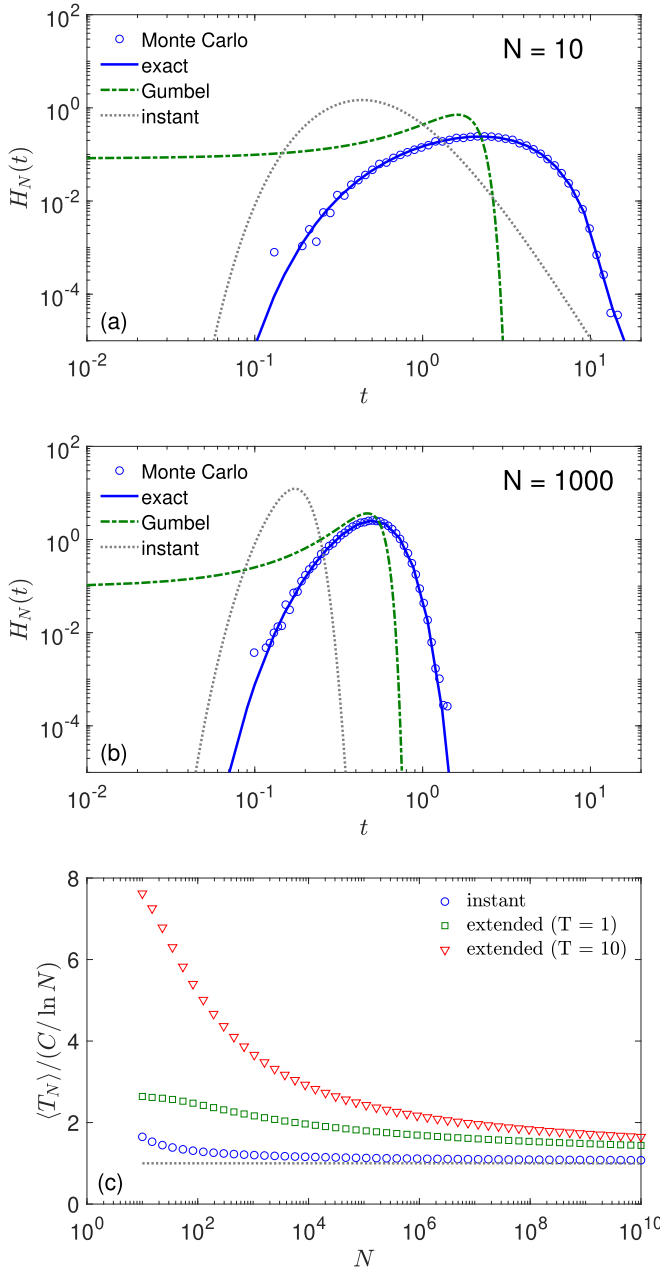
FIG. 8. (a), (b) PDF $H_N(t)$ of the fastest FPT $\mathcal{T}_N$ for diffusion on the half-line with $x_0 = 2$ and $D = 1$, and an extended injection modeled by the uniform distribution (D1) with $T = 10$, for (a) $N = 10$ and (b) $N = 1000$. The circles represent rescaled histograms obtained by generating $\mathcal{T}_N$ (with 10^5 realizations). The solid line represents the exact solution $H_N(t) = N H_\psi(t)[S_\psi(t)]^{N-1}$, where $S_\psi(t)$ and $H_\psi(t)$ are given by Eqs. (D2) and (D5). The dash-dotted line represents the asymptotic Gumbel distribution, with the scale and location parameters a_N and b_N given by Eq. (C2) with the parameters in Eq. (D4). The dotted line indicates the exact density for an instantaneous injection. (c) Mean fFPT $\langle \mathcal{T}_N \rangle$, rescaled by $C/\ln N$, as a function of N for diffusion on the half-line, with $x_0 = 2$ and $D = 1$, for an instantaneous injection (circles) and an extended injection of N particles modeled by the uniform distribution (D1) with $T = 1$ (squares) and $T = 10$ (triangles). The mean fFPTs were obtained from numerically computing the integral in Eq. (15). The dotted line indicates the constant 1 to highlight the approach to the leading-order term $C/\ln N$.
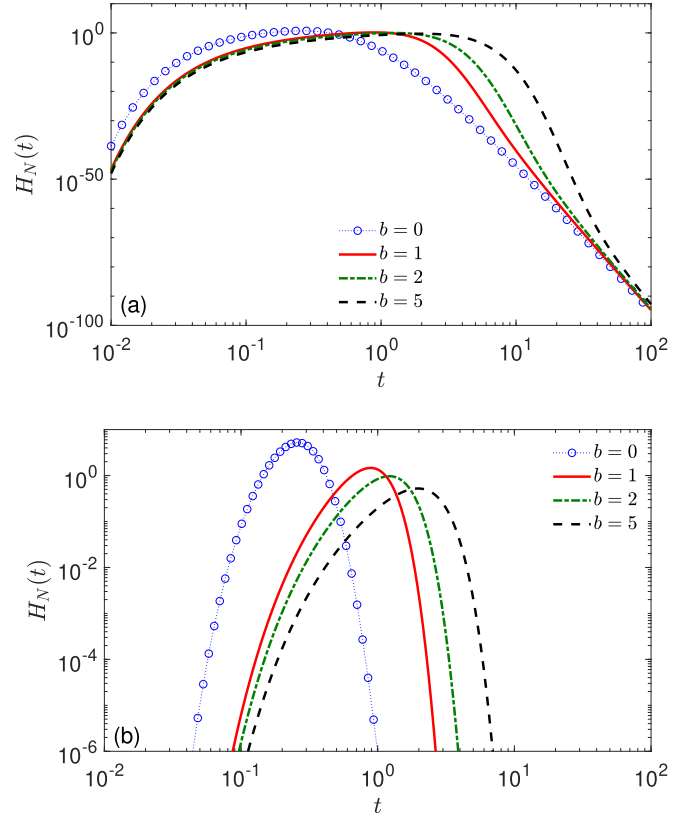

FIG. 9. PDF $H_N(t)$ of the fastest FPT $\mathcal{T}_N$ for diffusion on the half-line, with $x_0 = 2$, $D = 1$, and $N = 100$, with an extended injection modeled by the gamma distribution (26) with $\nu = 2$ and four values of b (see the legend; note that $b = 0$ formally corresponds to an instantaneous injection). (a) Full plot; (b) Zoom into the vertical axis from 10^{-6} to 10^1.

APPENDIX E: SUPPLEMENTARY ILLUSTRATION

In this Appendix, we provide a supplementary illustration to the numerical results presented in the main text.

Figure 9 shows how the PDF $H_N(t)$ is affected by the timescale b of the gamma distribution (26) of the entrance times. In Fig. 9(a), one can see that both the left and the right tails of the PDF are independent of b in the limits $t \to 0$ and $t \to \infty$. However, all curves start to follow the same asymptotic behavior at extremely small amplitudes ($\sim 10^{-100}$), which are totally irrelevant for applications. In turn, the relevant range of the amplitudes can be obtained by zooming into this plot, as shown in Fig. 9(b). Expectedly, an increase of b implies longer entrance times and thus shifts the PDF to the right.

APPENDIX F: ANALYSIS OF THE MOST PROBABLE TIME

The most probable time T_{mp} characterizes the maximum of the PDF and can thus be found by solving the equation

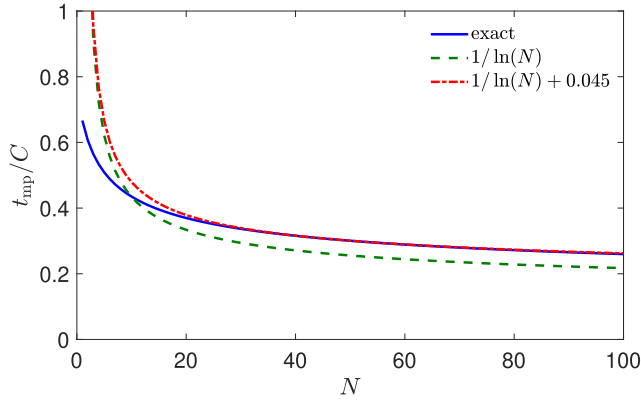$$\partial_t H_N(t) = N[S(t)]^{N-2}(S(t)\partial_t H(t) - (N-1)[H(t)]^2) = 0,$$
(F1)

FIG. 10. Most probable time T_{mp} [divided by $C = x_0^2/(4D)$] for diffusion on the half-line with an instantaneous injection of N particles. The solid line represents the exact value obtained by solving numerically Eq. (F4); the dashed and dash-dotted lines show two approximate asymptotic relations, $1/\ln(N)$ and $1/\ln(N) + 0.045$, the second one being shifted for a better agreement.

which leads to

$$\partial_t \ln(H(t)) = (N-1)\frac{H(t)}{S(t)}. \tag{F2}$$

For diffusion on the half-line, we substitute expressions for $H(t)$ and $S(t)$ to find

$$N - 1 = f(\xi), \tag{F3}$$

where $\xi = t/C$, $C = x_0^2/(4D)$ and

$$f(\xi) = \frac{\sqrt{\pi}\,\mathrm{erf}(\sqrt{1/\xi})\left(1 - \frac{3}{2}\xi\right)}{\sqrt{\xi}}e^{1/\xi}. \tag{F4}$$

One can check that $f(\xi)$ is a monotonously decreasing function of ξ which diverges as $\xi \to 0$ and vanishes at $\xi = 2/3$. In a first approximation, one can neglect slowly varying functions (as compared to $e^{1/\xi}$) to get $N - 1 \approx \sqrt{\pi}e^{1/\xi}$, from which

$$\xi \approx \frac{1}{\ln((N-1)/\sqrt{\pi})}. \tag{F5}$$

Higher-order corrections (accounting for $1/\sqrt{\xi}$) are needed to get the correct asymptotic behavior. Nevertheless, we see that, in our rough approximation,

$$T_{\mathrm{mp}} \approx \frac{C}{\ln N} = \frac{x_0^2}{4D \ln N}, \tag{F6}$$

i.e., the most probable time behaves similarly as the mean FPT. This approximation can be further improved, as illustrated in Fig. 10.

[1] K. Reynaud, Z. Schuss, N. Rouach, and D. Holcman, Why so many sperm cells? Commun. Integr. Biol. **8**, e1017156 (2015).

[2] M. Klinger-Strobel, H. Suesse, D. Fischer, M. W. Pletz, and O. Makarewicz, A novel computerized cell count algorithm for biofilm analysis, PLoS One **11**, e0154937 (2016).

[3] H.-C. Flemming and S. Wuertz, Bacteria and archaea on Earth and their abundance in biofilms, Nat. Rev. Microbiol. **17**, 247 (2019).

[4] G. L. Fain, *Molecular and Cellular Physiology of Neurons* (Harvard University Press, Cambridge, MA, 1999).

[5] B. Hille, *Ion Channels of Excitable Membranes* (Sinauer Associates, Sunderland, MA, 2001).

[6] B. Alberts, D. Bray, J. Lewis, M. Raff, K. Roberts, and J. D. Watson, *Molecular Biology of the Cell*, 3rd ed. (Garland, New York, NY, 1994).

[7] D. Grebenkov, R. Metzler and G. Oshanin, Eds., *Target Search Problems* (Springer, Cham, 2024).

[8] G. H. Weiss, K. E. Shuler, and K. Lindenberg, Order statistics for first passage times in diffusion processes, J. Stat. Phys. **31**, 255 (1983).

[9] B. Meerson and S. Redner, Mortality, redundancy, and diversity in stochastic search, Phys. Rev. Lett. **114**, 198101 (2015).

[10] Z. Schuss, K. Basnayake and D. Holcman, Redundancy principle and the role of extreme statistics in molecular and cellular biology, Phys. Life Rev. **28**, 52 (2019).

[11] K. Basnayake, Z. Schuss and D. Holcman, Asymptotic formulas for extreme statistics of escape times in 1, 2 and 3-dimensions, J. Nonlinear Sci. **29**, 461 (2019).

[12] S. D. Lawley, Distribution of extreme first passage times of diffusion, J. Math. Biol. **80**, 2301 (2020).

[13] S. D. Lawley and J. B. Madrid, A probabilistic approach to extreme statistics of Brownian escape times in dimensions 1, 2, and 3, J. Nonlinear Sci. **30**, 1207 (2020).

[14] S. D. Lawley, Universal formula for extreme first passage statistics of diffusion, Phys. Rev. E **101**, 012413 (2020).

[15] J. B. Madrid and S. D. Lawley, Competition between slow and fast regimes for extreme first passage times of diffusion, J. Phys. A: Math. Theor. **53**, 335002 (2020).

[16] D. S. Grebenkov, R. Metzler, and G. Oshanin, From single-particle stochastic kinetics to macroscopic reaction rates: Fastest first-passage time of N random walkers, New J. Phys. **22**, 103004 (2020).

[17] S. D. Lawley, Competition of many searchers, *in Target Search Problems,* edited by D. Grebenkov, R. Metzler, and G. Oshanin (Springer, Cham, 2024), p. 281.

[18] D. S. Grebenkov, R. Metzler, and G. Oshanin, Search efficiency in the Adam-Delbrück reduction-of-dimensionality scenario versus direct diffusive search, New J. Phys. **24**, 083035 (2022).

[19] O. Pulkkinen and R. Metzler, Distance matters: The impact of gene proximity in bacterial gene regulation, Phys. Rev. Lett. **110**, 198101 (2013).

[20] J. Elf, G.-W. Li, and X. S. Xie, Probing transcription factor dynamics at the single-molecule level in a living cell, Science **316**, 1191 (2007).

[21] T. E. Kuhlman and E. C. Cox, Gene location and DNA density determine transcription factor distributions in *Escherichia coli*, Mol. Syst. Biol. **8**, 610 (2012).

[22] R. Arbel-Goren, S. A. McKeithen-Mead, D. Voglmaier, I. Afremov, G. Teza, A. D. Grossmann, and J. Stavans, Target search by an imported conjugative DNA element for a unique integration site along a bacterial chromosome during horizontal gene transfer, Nucl. Acids Res. **51**, 3116 (2023).

[23] M. Ptashne and A. Gann, *Genes and Signals* (Cold Spring Harbor Laboratory Press, Cold Spring Harbor, NY, 2002).

[24] A. Zilman, Effects of multiple occupancy and interparticle interactions on selective transport through narrow channels: Theory versus experiment, Biophys. J. **96**, 1235 (2009).

[25] T. Zheng and A. Zilman, Kinetic cooperativity resolves bidirectional clogging within the nuclear pore complex, Biophys. J. **123**, 1085 (2024).

[26] A. L. Hodgkin and A. F. Huxley, A quantitative description of membrane current and its application to conduction and excitation in nerve, J. Physiol. **117**, 500 (1952).

[27] J. Sheng, L. He, H. Zheng, L. Xue, F. Luo, W. Shin, T. Sun, T. Kuner, D. T. Yue, and L.-G. Wu, Calcium-channel number critically influences synaptic strength and plasticity at the active zone, Nat. Neurosci. **15**, 998 (2012).

[28] Y. Nakamura, H. Harada, N. Kamasawa, K. Matsui, J. S. Rothman, R. Shigemoto, R. A. Silver, D. A. DiGregorio, and T. Takahashi, Nanoscale distribution of presynaptic Ca^{2+} channels and its impact on vesicular release during development, Neuron **85**, 145 (2015).

[29] J. Brockhaus, B. Brüggen and M. Missler, Imaging and analysis of presynaptic calcium influx in cultured neurons using synGCaMP6f, Front. Synaptic Neurosci. **11**, 12 (2019).

[30] M. Reva, D. A. DiGregorio, and D. S. Grebenkov, A first-passage approach to diffusion-influenced reversible binding: Insights into nanoscale signaling at the presynapse, Sci. Rep. **11**, 5377 (2021).

[31] D. Campos and V. Méndez, Dynamic redundancy as AI mechanism to optimize collective random searches, Phys. Rev. E **109**, 064109 (2024).

[32] H. Meyer and H. Rieger, Optimal number of agents in a collective search and when to launch them, arXiv:2401.05851 [Phys. Rev. E (to be published)].

[33] D. S. Dimitrov, Virus entry: Molecular mechanisms and biomedical applications, Nat. Rev. Microbiol. **2**, 109 (2004).

[34] A. J. Bray, S. N. Majumdar and G. Schehr, Persistence and first-passage properties in nonequilibrium systems, Adv. Phys. **62**, 225 (2013).

[35] T. Agranov and B. Meerson, Narrow escape of interacting diffusing particles, Phys. Rev. Lett. **120**, 120601 (2018).

[36] B. Meerson and G. Oshanin, Geometrical optics of large deviations of fractional Brownian motion, Phys. Rev. E **105**, 064137 (2022).

[37] J. Casas-Vàzquez, D. Jou, and G. Lebon, *Extended Irreversible Thermodynamics* (Springer-Verlag, Berlin, 1996).

[38] G. Cattaneo, Sulla conduzione del calore [On the conduction of heat], Atti. Sem. Mat. Fis. Univ. Modena **3**, 83 (1948).

[39] R. Corless, G. Gonnet, D. Hare, D. Jeffrey, and D. Knuth, On the Lambert function, Adv. Comput. Math. **5**, 329 (1996).